Regular Article

Design, Synthesis and Biological Evaluation of Oxindole-Based Chalcones as Small-Molecule Inhibitors of Melanogenic Tyrosinase

Sharad Kumar Suthar,[a] Sumit Bansal,[a] Niteen Narkhede,[a] Manju Guleria,[b] Angel Treasa Alex,[c] and Alex Joseph*,[a]

[a] *Department of Pharmaceutical Chemistry, Manipal College of Pharmaceutical Sciences; Manipal-576104, India:* [b] *School of Pharmaceutical Sciences, Jaipur National University; Jaipur-302017, India: and* [c] *Department of Pharmaceutical Biotechnology, Manipal College of Pharmaceutical Sciences; Manipal-576104, India.*
Received April 11, 2017; accepted June 2, 2017

The enzyme tyrosinase regulates melanogenesis and skin hyperpigmentation by converting L-3,4-dihydroxyphenylalanine (L-DOPA) into dopaquinone, a key step in the melanin biosynthesis. The present work deals with design and synthesis of various oxindole-based chalcones as monophenolase and diphenolase activity inhibitors of tyrosinase. Among the screened compounds, 4-hydroxy-3-methoxybenzylidene moiety bearing chalcone (7) prepared by one pot reaction of oxindole and vanillin displayed the highest activity against tyrosinase with IC_{50}s of 63.37 and 59.71 μM in monophenolase and diphenolase activity assays, respectively. In molecular docking studies, chalcone 7 also showed the highest binding affinity towards the enzyme tyrosinase while exhibiting the lowest estimated free energy of binding, among all the ligands docked.

Key words tyrosinase inhibitor; oxindole-based chalcone; melanogenesis; molecular docking

Tyrosinase is a major enzyme of melanogenic cascade, accountable for hydroxylation of L-tyrosine to L-3,4-dihydroxyphenylalanine (L-DOPA) and subsequent oxidation of L-DOPA to dopaquinone, the significant steps in melanin production.[1,2] Melanogenesis is a major defence mechanism of human skin against UV radiations. However, abnormal production and accumulation of melanin in the skin are a serious aesthetic problem, which can cause melasma, freckles, ephelide, and senile lentigines.[3] In the food industry, melanin is responsible for browning reactions in fruits and vegetables, resulting in the nutritional as well as market value loss. Therefore, the development of tyrosinase inhibitors has gradually become more important as skin whitening agents and preservatives in cosmetic and food industry, respectively,[4,5] and research in this area is continuously growing.[6–13] Many tyrosinase inhibitors have already been reported from both synthetic and natural sources, for example hydroquinone, kojic acid, arbutin, retinol, linoleic acid, galangin, and numerous botanical products.[14] However, due to undesirable side effects, many of them are banned in several countries.[15,16]

The indole moiety is considered as a promising scaffold for tyrosinase inhibition[17] and many indole group bearing compounds, such as *N*-*p*-coumaroyl serotonin, *N*-feruloyl serotonin, and *N*-caffeoyl serotonin have been described as potential tyrosinase inhibitors.[18] Likewise, octapeptide containing indole scaffold has also been reported as a strong inhibitor of tyrosinase.[19] The role of indole moiety and tyrosinase in melanogenesis has been depicted in Fig. 1. In the similar vein, α,β-unsaturated carbonyl compounds, the chalcones are known to possess diverse biological activities, *e.g.* antioxidant,[20] anticancer,[21] anti-inflammatory,[22] antidepressive,[23] antimicrobial,[24] and anti-tyrosinase.[25,26] Isoliquiritigenin chalcone as a potent inhibitor of tyrosinase was reported by Nerya *et al.*[25] Recently, we reported (*Z*)-3-(2,4,6-trihydroxybenzylidene)-indolinone that suppressed the tyrosinase activity in a double-digit micro-molar range.[26] Many other studies have also confirmed the tyrosinase inhibitory potential of chalcones, which can be attributed to their antioxidant capability suppressing the pigmentation resulting from auto-oxidative process.[27,28] Furthermore, Okombi *et al.*[29] published the report of benzylidenebenzofuran-3(2*H*)-ones as inhibitors of tyrosinase from human melanocytes. The lead compound (*Z*)-4,6-dihydroxy-2-(4-hydroxybenzylidene)benzofuran-3(2*H*)-one displayed an IC_{50} of 38±2.9 μM, emerging as the remarkably potent inhibitor of tyrosinase when compared with the reference compound kojic acid. The pharmacophoric similarity between the lead tyrosinase inhibitor (*Z*)-4,6-dihydroxy-2-(4-hydroxybenzylidene) benzofuran-3(2*H*)-one and our synthesized compounds (**3**–**10**) has been presented in Fig. 2. Based on these remarks, we synthesized oxindole-based chalcones to investigate their tyrosinase inhibitory potential for their applications as skin whitening agents in cosmetics and as preservatives in food industry.

Results and Discussion

Chemistry The synthesis of oxindole-based chalcones (**3**–**10**) was carried out by Claisen–Schmidt condensation reaction of a ketone with various aldehydes. Oxindole (indolin-2-one) (**1**) was stirred with appropriate aldehydes (**2**) in the presence of ethanolic NaOH to yield the title compounds (**3**–**10**) (Chart 1). All the compounds were synthesized in fairly good yields (75–94%) and their structures were established by using UV, IR, ^{1}H-NMR, and mass spectroscopic techniques. The UV spectra of compounds (**3**–**10**) demonstrated two typical chalcone bands, the band-I at 441.50–347.00 nm and band-II at 270.50–239.50 nm. The IR spectra of compounds (**3**–**10**) displayed peaks at 3143.97–3192.19, 1616.35–1699.29, and 1564.27–1614.42 cm^{-1} distinctive to N–H group and α,β-unsaturated carbonyl system, *i.e.* C=O and C=C groups, respectively. The ^{1}H-NMR spectra of synthesized compounds showed two singlets at 9.0202–11.8558 and 7.2566–8.3317 ppm characteristic to N<u>H</u> and=C<u>H</u> (vinylic) protons, respectively.

* To whom correspondence should be addressed. e-mail: alex.joseph@manipal.edu

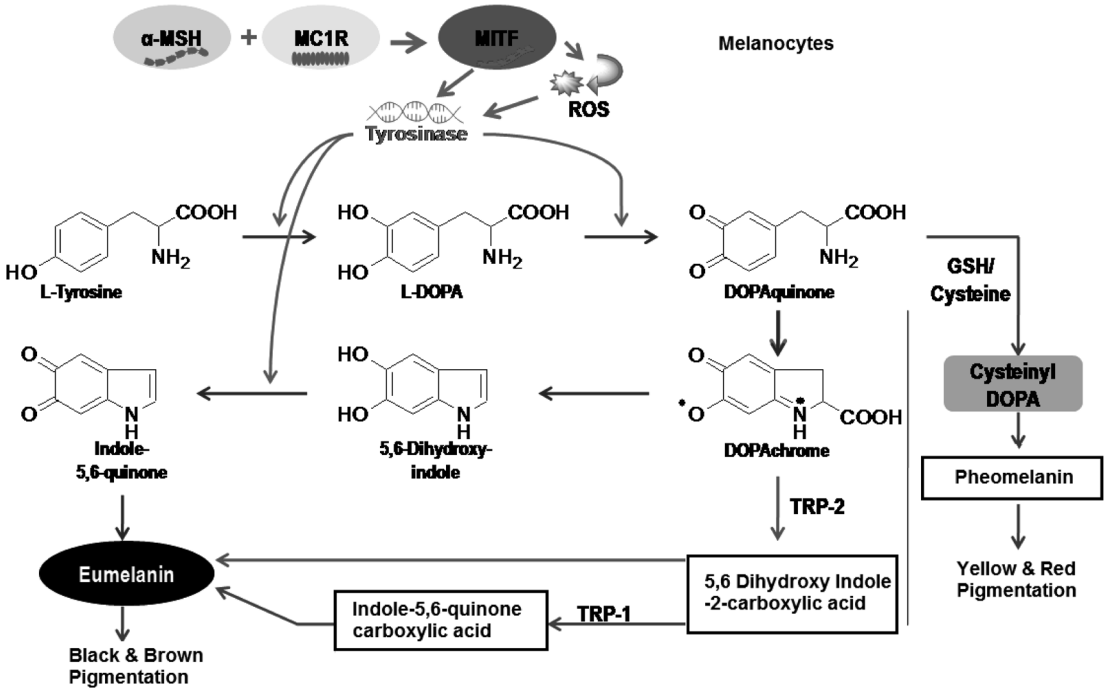

Fig. 1. Role of Indole Moiety and Tyrosinase in Melanogenic Pathway

α-MSH; α-melanocyte-stimulating harmone, MC1R; melanocortin 1 receptor, MITF; microphthalamia-associated transcription factor, ROS; reactive oxygen species, TRP; tyrosinse-related proteins.

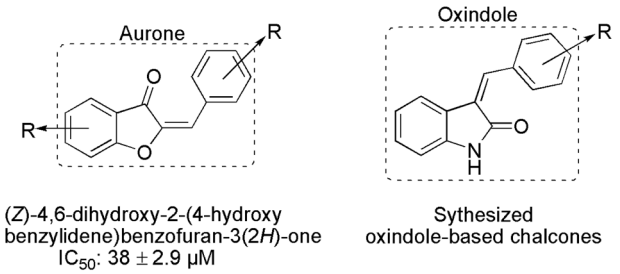

Fig. 2. Pharmacophoric Similarity between the Lead Tyrosinase Inhibitor (*Z*)-4,6-Dihydroxy-2-(4-hydroxybenzylidene)benzofuran-3(2*H*)-one of Aurone Class and Synthesized Oxindole-Based Chalcones

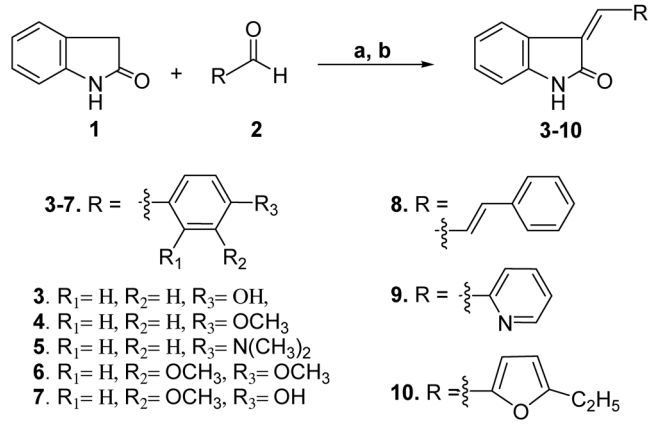

(a) Ethanolic NaOH; (b) Stir 2 h.

Chart 1. Synthesis of New Oxindole-Based Chalcones (**3**–**10**)

However, in the ^{1}H-NMR spectrum of 3-phenylallylidene substituted compound **8**, =CH proton appeared upfield and as a doublet due to the presence of neighbouring Ar-CH=CH-group. The total number of protons in the ^{1}H-NMR spectra of compounds were consistent with their respective protons of molecular formulas. The high resolution (HR)-MS electrospray ionization (ESI)-MS spectra of compounds displayed molecular ion peaks distinctive to their molecular masses. Taken together, the structures of synthesized *α*,*β*-unsaturated carbonyl compounds (**3**–**10**) were confirmed by the presence of IR and NMR peaks characteristic to *α*,*β*-unsaturation, along with the presence of molecular ion peaks corresponding to the molecular masses of the synthesized compounds.

Table 1. Tyrosinase Inhibition Activity of Oxindole-Based Chalcones (**3**–**10**)

Compound	IC_{50} (μM)	
	L-Tyrosine	L-DOPA
3	**77.07**	**85.33**
4	152.88	145.17
5	256.70	241.89
6	182.46	180.25
7	**63.37**	**59.71**
8	223.56	232.32
9	**95.98**	**99.10**
10	110.77	107.26
Kojic acid	22.52	29.74

Tyrosinase Inhibition Activity The tyrosinase inhibitory activity of oxindole-based chalcones (**3**–**10**) and reference compound kojic acid was investigated by using L-tyrosine and L-DOPA as the substrates in monophenolase and diphenolase activity assays, respectively. The results obtained in these assays are shown in Table 1 and Fig. 3.

Among the chalcones evaluated, compound **3** (4-hydroxy substituted) and **7** (4-hydroxy-3-methoxy substituted) ex-

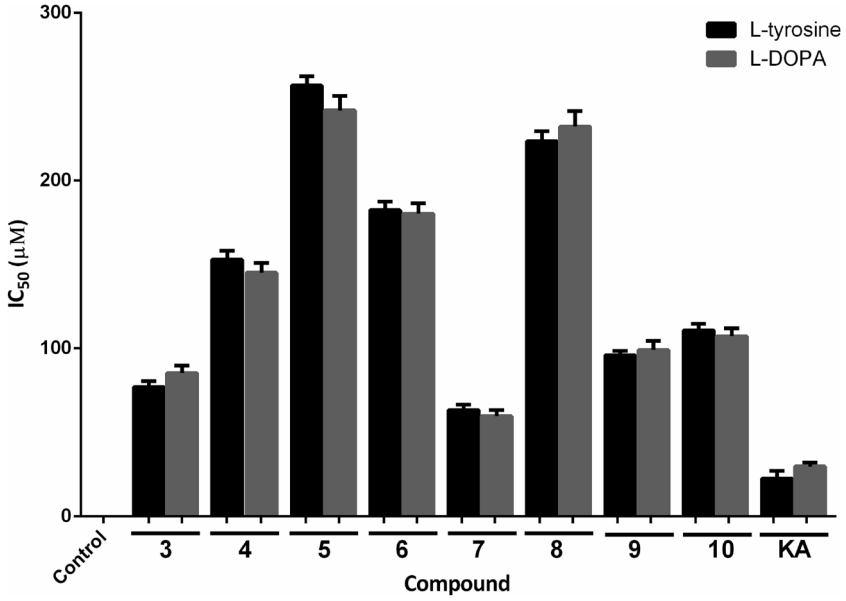

Fig. 3. IC_{50} (μM) Plot of Oxindole-Based Chalcones and Reference Compound Kojic Acid for Tyrosinase Inhibition

Results presented are mean±S.E.M. of three values.

hibited the most potent tyrosinase inhibitory activity with IC_{50}s of 77.07 and 63.37 μM in monophenolase and 85.33 and 59.71 μM in diphenolase activity assays, respectively. At the same time, the reference compound kojic acid demonstrated 50% of tyrosinase inhibition at concentrations of 22.52 and 29.74 μM in monophenolase and diphenolase activity assays, correspondingly. It is evident from the results that the hydroxyl group bearing compounds **3** and **7** displayed IC_{50}s much comparable to that of the reference compound kojic acid. On the other hand, compounds **4** and **6** lacking a hydroxyl group at position-4 of benzylidene moiety, showed moderate to poor activity (IC_{50}s of 152.88 and 182.46 μM in monophenolase and 145.17 and 180.25 μM in diphenolase activity assays, respectively). These results indicate the importance of a hydroxyl group at position 4 of benzylidene moiety for tyrosinase inhibition. However, a complete loss of activity was observed in 4-dimethylamino substituted compound **5** (neither hydroxylated nor methoxylated at position 4). Upon comparison between the inhibitory potential of compounds **3** and **7**, we found that the methoxy group at position 3 of the benzylidene ring in compound **7** augments the tyrosinase inhibition. In addition, 3-phenylallylidene substituted compound **8** (chalcone prepared by reaction of cinnamaldehyde with oxindole) showed the least activity against tyrosinase; and thus, it may be assumed that this modification is not useful for the inhibition of tyrosinase. On the contrary, chalcone prepared from heterocyclic aldehydes, such as **9** (2-pyridinecarboxaldehyde) and **10** (5-ethylfurfural) exhibited moderate tyrosinase inhibitory potential with IC_{50}s of 95.98 and 110.77 μM in monophenolase and 99.10 and 107.26 μM in diphenolase activity assays, respectively. These results indicated that the replacement of benzylidene scaffold with 5 or 6 membered heterocyclic counterparts may retain the tyrosinase inhibitory potential of oxindole-based chalcones.

While discussing the mode of tyrosinase inhibition by our lead compound **7** or other chalcones, since our designed compounds are based on mimicking the structural part of tyrosinase substrates (Fig. 1); (i) L-tyrosinse, (ii) L-DOPA, and 5,6-dihydroxyindole, we can accept that these compounds will act as competitive inhibitors of tyrosinase. Moreover, many previous studies have already reported that chalcones which bear the structural similarity with tyrosinase substrates act as the competitive inhibitors of the enzyme.[28,30]

Molecular Docking Analysis Before performing molecular docking studies, all the designed chalcones were assessed against the Lipinski's Rule of Five[31] and other drug-likeness parameters. The Lipinski's Rule of Five states that for a chemical compound to be a successful oral drug, it should not violate more than one of the following parameters; i) Number of hydrogen bond donors (sum of OHs and NHs) should be $\leq$5, ii) Number of hydrogen bond acceptors (sum of Os and Ns) should be $\leq$10, iii) Its Log$P$ value should be $\leq$5, iv) Its molecular weight should be $\leq$500. The calculation of Lipinski's Rule of Five along with molar refractivity and polar surface area parameters revealed that none of the designed chalcones violated these drug-likeness parameters. Moreover, all the compounds demonstrated the values well within the proposed limits of parameters as shown in Table 2.

In order to predict the possible binding interactions that might take place between the oxindole-based chalcones and tyrosinase enzyme, all the designed compounds were docked into the active site of tyrosinase. These docked compounds showed estimated free energy of binding in the range of –7.09 to −1.18 kcal/mol (Table S1). Among them, 4-hydroxy-3-methoxybenzylidene moiety bearing compound **7** showed the lowest estimated free energy of binding, whereas 4-dimethylaminobenzylidene moiety possessing compound **5** exhibited the highest estimated free energy of binding. Closer analysis of the docked complex formed between compound **7** and tyrosinase indicated the presence of three strong hydrogen bonds; where, two bondings were of 1.8 Å each, while another one was of 2.2 Å (Figs. 4, 5). The hydroxyl oxygen of benzylidene scaffold was hydrogen bonded with the histidine (His)-60 (H–O…H–N, 1.8 Å), while carbonyl oxygen of oxindole moiety was interacting with the valine (Val)-218 (C=O…H–N, 1.8 Å) residue of tyrosinase. Additionally, the hydroxyl oxygen

Table 2. Calculation of Lipinski's Rule of Five and Other Descriptors for Synthesized Oxindole-Based Chalcones

Compd.	No. of H-bond donors	No. of H-bond acceptors	Log *P*	Molecular weight	Molar refractivity (cm^3)	Polar surface area ($Å^2$)	Lipinski's & other violations
3	2	2	2.96	237.25	71.71	49.33	0
4	1	2	3.11	251.28	76.19	38.33	0
5	1	2	3.37	264.32	84.16	32.34	0
6	1	3	2.95	281.31	82.66	47.56	0
7	2	3	**2.80**	267.28	78.18	**58.56**	0
8	1	1	3.79	247.29	80.05	29.10	0
9	1	2	2.28	222.24	67.13	41.99	0
10	1	1	3.05	239.27	71.80	42.24	0

No. of H-bond donors ≤5. No. of H-bond acceptors ≤10. Log *P* ≤5. Molecular weight ≤500. Molar refractivity 30–140 cm^3. Polar surface area ≤140 $Å^2$.

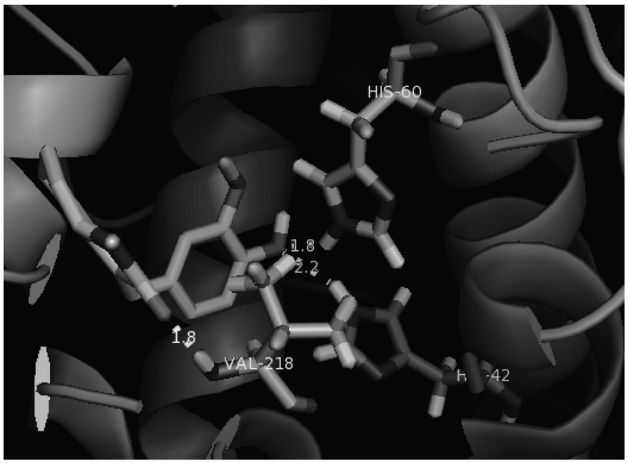

Fig. 4. Molecular Docking of the Lead Compound **7** in the Active Site of Tyrosinase

The amino acids His-42, His-60, and Val-218 involved in hydrogen bond interactions with the compound **7** are highlighted.

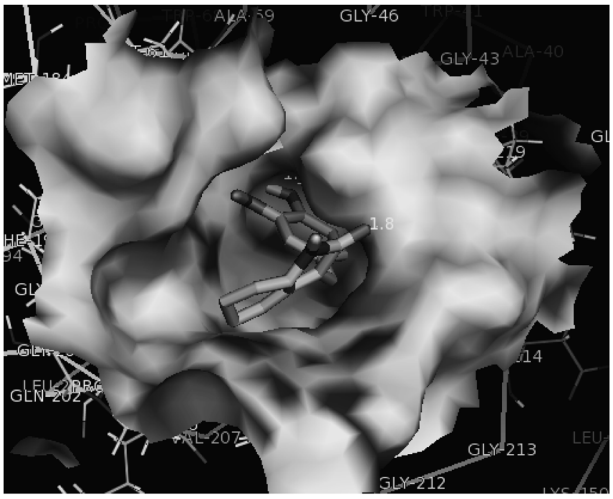

Fig. 5. 3D Binding Orientation of the Lead Compound **7** in the Active Site of Tyrosinase

of benzylidene also formed a hydrogen bond with the His-42 residue (H–O…H–N, 2.2 Å) of the target protein. Apart from hydrogen bondings, the oxindole scaffold of compound **7** was positioned in the hydrophobic cavity created by Val-217, Val-218, and proline (Pro)-219 residues of tyrosinase (Fig. 6). Further analyses of the docked complex indicated hydrophobic and van der Waals contacts between the benzylidene part of compound **7** and methionine (Met)-61, phenylalanine (Phe)-65, leucine (Leu)-66, Phe-197 residues of tyrosinase (Fig. 6).

Taken together, the formation of three strong hydrogen bonds between compound **7** and tyrosinase (His-42, His-60, and Val-218 residues were involved) and deep positioning of oxindole scaffold in the hydrophobic pocket of Val-217, Val-218, and Pro-219 residues might have played a central role in the tyrosinase inhibitory activity of the lead compound **7**. Furthermore, the lead compound **7** has the highest polar surface area and second least Log *P* value among all the compounds synthesized. The compound **7** was further analysed for absorption, distribution, metabolism, excretion, and toxicity (ADMET) parameters and results of this study have been summarized in Table 3.

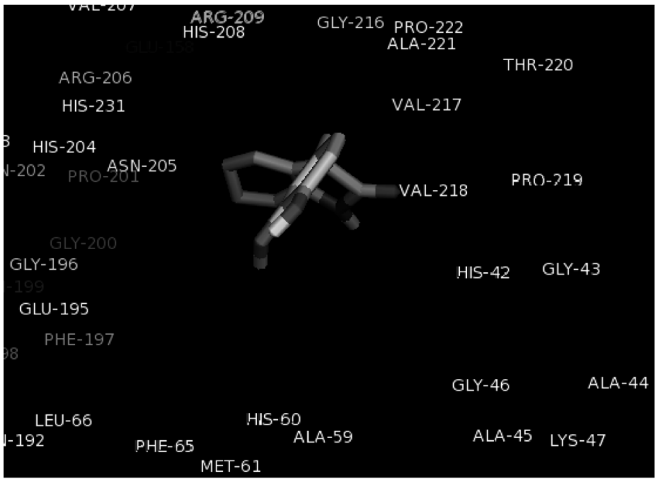

Fig. 6. Molecular Docking of the Lead Compound **7** in the Active Site of Tyrosinase

The amino acids involved in hydrogen, hydrophobic, and van der Waals interactions and present in the surroundings of compound **7** are highlighted.

Conclusion In the present study, we report for the first time, the potential of oxindole-based chalcones as tyrosinase inhibitors. The results of this study concluded that the type and position of substitutions on benzylidene moiety are fundamental for the oxindole-based chalcones to impart tyrosinase inhibitory activity. Among the synthesized chalcones, compound **7** was emerged as the most potent tyrosinase inhibitor that possessed a hydroxyl group at position 4 and a methoxy group at position 3 of benzylidene moiety. In conclusion, this work offers an oxindole-based new scaffold for the develop-

Table 3. Prediction of ADMET Profile of the Lead Compound **7**

Parameter	Compound **7** (Most active)	
Absorption		
	Result	Probability
Blood–Brain Barrier	BBB^+	0.7717
Human Intestinal Absorption	HIA^+	1.0000
Caco-2 Permeability ($\log P_{app}$, cm/s)	Caco-2^+	0.6196
P-Glycoprotein Substrate	Substrate	0.5596
P-Glycoprotein Inhibitor	Non-inhibitor	0.7554
Renal Organic Cation Transporter	Non-inhibitor	0.8349
Distribution and Metabolism		
CYP450 2C9 Substrate	Non-substrate	0.7888
CYP450 2D6 Substrate	Non-substrate	0.7348
CYP450 3A4 Substrate	Substrate	0.6051
CYP450 1A2 Inhibitor	Inhibitor	0.9099
CYP450 2C9 Inhibitor	Inhibitor	0.7704
CYP450 2D6 Inhibitor	Non-inhibitor	0.7813
CYP450 2C19 Inhibitor	Non-inhibitor	0.7095
CYP450 3A4 Inhibitor	Inhibitor	0.7457
CYP Inhibitory Promiscuity	High	0.8324
Excretion and Toxicity		
AMES Toxicity	Toxic	0. 8277
Carcinogens	Non-carcinogens	0.9422
Acute Oral Toxicity	III	0.4339
Rat Acute Toxicity (LD_{50}, mol/kg)	2.6961	—

Acute Oral Toxicity: Category III includes compounds with LD_{50} values greater than 500 mg/kg but less than 5000 mg/kg. Probability indicates scale between 0 and 1.

ment of effective skin whitening agents. However, further research is required to optimize the lead and to understand the detailed molecular mechanism behind the tyrosinase inhibitory activity of these chalcones.

Experimental

Chemistry All the chemicals and reagents were purchased from Sigma-Aldrich, Aldrich, Merck, Ranbaxy Fine Chemicals Ltd., Sulabh Laboratories, and Spectrochem, India, and were used without further purification. Tyrosinase, L-tyrosine, L-DOPA, and kojic acid were purchased from Sigma Life Science, India. Melting points were recorded on a capillary melting point apparatus (Shital Scientific Industries, India) and are uncorrected. The UV-visible spectra were obtained with a Shimadzu UV-2450 spectrophotometer (Shimadzu, Japan). The IR spectra were recorded on a Shimadzu FTIR-8310 (Shimadzu) using potassium bromide discs. The proton NMR spectra were recorded on a Bruker AVANCE II 400 MHz spectrophotometer (Bruker, Germany) and chemical shifts are reported in parts per million (δ). The proton NMR spectra in the supplementary data file were prepared with Mnova 8.1.1 program of Mastrelab Research, Spain by processing flame ionization detecter (FID) files of earlier mentioned Bruker NMR instrument. The mass spectra (ESI-HR-MS) were obtained with a Bruker, Compact, Qq-TOF LC-MS/MS mass spectrometer (Bruker, Germany). Elemental analysis was performed on a 2400 CHN analyzer (PerkinElmer, Inc., U.S.A.). The purity of all the compounds was established by a single spot on the TLC silica gel $60F_{254}$ plates (Merck, Germany). The *n*-hexane: ethyl acetate (7 : 3) solvent system was used a mobile phase in TLC.

General Procedure for the Synthesis of Compounds (3–10) Oxindole (0.1 mol, 1.33 g) (**1**) and appropriate aldehyde (0.1 mol) (**2**) in an ethanolic solution (80%, 25 mL) containing 2% sodium hydroxide were stirred in ice-cold conditions for about 2 h (Chart 1). The reaction mixture was kept in the refrigerator for about 10–12 h followed by neutralized with 20% HCl solution with continuous stirring. The solid product precipitated out was filtered off, washed with ample water, and dried to yield a final purified product.

(*Z*)-3-(4-Hydroxybenzylidene)indolin-2-one (3) Light-yellow solid; Yield: 87%; mp: 285–286°C; UV λ_{max} (MeOH) nm: 351.50, 246.50. IR (KBr) cm^{-1}: 3234.62 (broad, O–H & N–H stretch), 3022.45, 2819.93 (C–H stretch), 1683.86 (C=O stretch), 1585.49 (C=C stretch). ^{1}H-NMR (mixture of $CDCl_3$ & dimethyl sulfoxide (DMSO)-d_6, 400 MHz) δ: 10.4766 (s, 1H, NH), 10.0758 (1H, s, OH), 7.5457 (s, 1H, =CH (C-11-H)), 6.8406–7.7174 (8H, Ar-H). HR-MS (ESI) *m/z*: 238.0860 $(M+1)^+$ (Calcd for $C_{15}H_{11}NO_2$: 237.0784). *Anal.* Calcd for $C_{15}H_{11}NO_2$: C, 75.94; H, 4.67; N, 5.90. Found: C, 75.99; H, 4.68; N, 5.87.

(*Z*)-3-(4-Methoxybenzylidene)indolin-2-one (4) Orange-red solid; Yield: 93%; mp: 99–100°C; UV λ_{max} (MeOH) nm: 347.00, 247.00. IR (KBr) cm^{-1}: 3192.19 (N–H stretch), 3072.60, 2962.66, 2837.29 (C–H stretch), 1697.36 (C=O stretch), 1606.70 (C=C stretch). ^{1}H-NMR ($CDCl_3$, 400 MHz) δ: 9.0202 (s, 1H, NH), 7.2598 (s, 1H, =CH (C-11-H)), 6.8674–7.7537 (8H, Ar-H), 3.8849 (s, 3H, OCH_3 (C-19-H)). HR-MS (ESI) *m/z*: 252.1027 $(M+1)^+$, 274.0844 $(M+Na)^+$ (Calcd for $C_{16}H_{13}NO_2$: 251.0941). *Anal.* Calcd for $C_{16}H_{13}NO_2$: C, 76.48; H, 5.21; N, 5.57. Found: C, 76.54; H, 5.19; N, 5.60.

(*Z*)-3-(4-(Dimethylamino)benzylidene)indolin-2-one (5) Orange-red solid; Yield: 82%; mp: 155–157°C; UV λ_{max} (MeOH) nm: 441.50, 270.50. IR (KBr) cm^{-1}: 3155.54 (N–H stretch), 3024.38, 2900.94, 2825.72, 2735.06 (C–H stretch), 1666.50 (C=O stretch), 1564.27 (C=C stretch). ^{1}H-NMR (mixture of $CDCl_3$ & DMSO-d_6, 400 MHz) δ: 10.3115 (s, 1H, NH), 7.4850 (s, 1H,=CH (C-11-H)), 6.7063–8.4245 (8H, Ar-H), 3.0795 & 3.0719 (singlet each, 6H, $N(CH_3)_2$). HR-MS (ESI) *m/z*: 265.1312 $(M+1)^+$, 287.1133 $(M+Na)^+$ (Calcd for $C_{17}H_{16}N_2O$: 264.1257). *Anal.* Calcd for $C_{17}H_{16}N_2O$: C, 77.25; H, 6.10; N, 10.60; Found: C, 77.21; H, 6.11; N, 10.62.

(*Z*)-3-(3,4-Dimethoxybenzylidene)indolin-2-one (6) Orange-yellow solid; Yield: 91%; mp: 179–180°C; UV λ_{max} (MeOH) nm: 366.00, 261.50 nm. IR (KBr) cm^{-1}: 3167.12 (N–H stretch), 3026.31, 2962.66, 2899.01, 2839.22 (C–H stretch), 1695.43 (C=O stretch), 1579.70 (C=C stretch). ^{1}H-NMR (mixture of $CDCl_3$ & DMSO-d_6, 400 MHz) δ: 10.4926 (s, 1H, NH), 7.6571 (s, 1H,=CH (C-11-H)), 6.8177–8.7319 (7H, Ar-H), 3.8771 (s, 3H, OCH_3), 3.8727 (s, 3H, OCH_3). HR-MS (ESI) *m/z*: 282.1106 $(M+1)^+$ (Calcd for $C_{17}H_{15}NO_3$: 281.1046). *Anal.* Calcd for $C_{17}H_{15}NO_3$: C, 72.58; H, 5.37; N, 4.98; Found: C, 72.62; H, 5.40; N, 4.97.

(*Z*)-3-(4-Hydroxy-3-methoxybenzylidene)indolin-2-one (7) Light-brown solid; Yield: 90%; mp: 220–221°C; UV λ_{max} (MeOH) nm: 371.00, 252.50. IR (KBr) cm^{-1}: 3396.64 (O–H stretch), 3174.83 (N–H stretch), 3072.60, 2835.36 (C–H stretch), 1685.79 (C=O stretch), 1587.42 (C=C stretch). ^{1}H-NMR (mixture of $CDCl_3$ & DMSO-d_6, 400 MHz) δ: 10.4926 (s, 1H, NH), 9.7266 (1H, s, OH), 7.5506 (s, 1H, =CH (C-11-H)), 6.8597–7.7796 (m, 7H, Ar-H), 3.8290 (s, 3H, OCH_3). HR-MS (ESI) *m/z*: 268.0968 $(M+1)^+$, 290.0796 $(M+Na)^+$ (Calcd for $C_{16}H_{13}NO_3$: 267.0890). *Anal.* Calcd for $C_{16}H_{13}NO_3$: C, 71.90; H, 4.90; N, 5.24; Found: C, 71.96; H, 4.89; N, 5.23.

(3*Z*)-3-((*E*)-3-Phenylallylidene)indolin-2-one (8) Orange-yellow solid; Yield: 94%; mp: 168–170°C; UV λ_{max} (MeOH) nm: 360.00, 239.50. IR (KBr) cm^{-1}: 3174.83 (N–H stretch), 3066.82, 3028.24, 2899.01, 2837.29 (C–H stretch), 1699.29 (C=O stretch), 1614.42, 1462.04 (C=C stretch). ^{1}H-NMR (mixture of $CDCl_3$ & DMSO-d_6, 400 MHz) δ: 10.4200 (s, 1H, NH), 7.1097–8.5353 (10H, Ar-H &=CH (C-11-H)), 6.9865–7.0242 (t, 1H, J=7.54 Hz, Ar-CHCH (C-12-H)), 6.8514–6.8706 (d, 1H, J=7.68 Hz, Ar-CHCH (C-13-H)). HR-MS (ESI) m/z: 248.1063 $(M+1)^+$, 270.0890 $(M+Na)^+$ (Calcd for $C_{17}H_{13}NO$: 247.0992). *Anal.* Calcd for $C_{17}H_{13}NO$: C, 82.57; H, 5.30; N, 5.66; Found: C, 82.55; H, 5.28; N, 5.65.

(*Z*)-3-((Pyridin-2-yl)methylene)indolin-2-one (9) Red solid; Yield: 75%; mp: 192–195°C; UV λ_{max} (MeOH) nm: 358.00, 260.00. IR (KBr) cm^{-1}: 3433.29 (N–H stretch), 3057.17, 2953.02, 2810.28, 2684.91 (C–H stretch), 1616.35 (C=O stretch), 1583.56 (C=C stretch). ^{1}H-NMR (mixture of $CDCl_3$ & DMSO-d_6, 400 MHz) δ: 11.8558 (s, 1H, NH), 8.3317 (s, 1H,=CH (C-11-H)), 7.0204–9.2271 (8H, Ar-H). HR-MS (ESI) m/z: 223.0843 $(M+1)^+$ (Calcd for $C_{14}H_{10}N_2O$: 222.0788). *Anal.* Calcd for $C_{14}H_{10}N_2O$: C, 75.66; H, 4.54; N, 12.60; Found: C, 75.71; H, 4.55; N, 12.58.

(*Z*)-3-((5-Ethylfuran-2-yl)methylene)indolin-2-one (10) Deep-yellow solid; Yield: 87%; mp: 190–191°C; UV λ_{max}(MeOH) nm: 368.50, 246.50. IR (KBr) cm^{-1}: 3143.97 (N–H stretch), 2972.31, 2883.58, 2804.50, 2630.91 (C–H stretch), 1658.78 (C=O stretch), 1610.56 (C=C stretch). ^{1}H-NMR (mixture of $CDCl_3$ & DMSO-d_6, 400 MHz) δ: 10.4677 (s, 1H, NH), 7.2566 (s, 1H, =CH (C-11-H)), 6.4170–8.3315 (6H, Ar- and furanyl-H), 2.8524–2.9090 (q, 2H, CH_2 (C-17-H)), 1.3211–1.3589 (t, 3H, J=7.56 Hz, CH_3 (C-18-H)). HR-MS (ESI) m/z: 240.1022 $(M+1)^+$, 262.0843 $(M+1+Na)^+$ (Calcd for $C_{15}H_{13}NO_2$: 239.0941). *Anal.* Calcd for $C_{15}H_{13}NO_2$: C, 75.30; H, 5.48; N, 5.85; Found: C, 75.37; H, 5.51; N, 5.82.

Tyrosinase Inhibition Assay Solutions of L-tyrosine/L-DOPA (0.9 mmol) and tyrosinase (13.8 units/mL) were prepared in 0.1 mol phosphate buffer of pH 6.8. The assay was carried out in a 96-well microtiter plate. Ten microliters of test or reference compound and 280 μL of L-tyrosine/L-DOPA solution were added to each well in triplicates. Then, 5 μL of tyrosinase solution was added to an each well. Control wells were loaded with 10 μL DMSO, 280 μL L-tyrosine/L-DOPA, and 5 μL of an enzyme. The plates were incubated at 25°C for 30 min. Following incubation, the amount of dopachrome generated was measured spectrophotometrically at 492 nm using microtiter plate reader. The IC_{50} was determined by interpolation of the dose–response curve using GraphPad Prism 6.0.

Molecular Descriptors, Molecular Docking, and ADMET Studies Molecular descriptors of compounds, including Lipinski's Rule of Five[31] were calculated by using MarvinSketch 6.3.1. For molecular docking studies, crystal structure of tyrosinase (PDB ID: 3NM8) was downloaded from the Protein Data Bank (PDB: http://www.pdb.org). Hetero atoms and water molecules were removed and hydrogens were added to protein for the correct calculation of partial atomic charges. The ligands to be docked were prepared in three dimensional (3D) format by using CS ChemDraw Ultra 8.0. The AutoDock tools 1.5.4 were used for molecular docking analysis. The grid box was positioned at 30, 42, and 24 Å (x, y and z) with center x=−11, y=12, and z=−8 and grid point spacing of 0.375 Å. The Lamarckian Genetic Algorithm (LGA) was applied to search conformers with lowest binding energy. Results of molecular docking studies are presented as estimated free energy of binding in kcal/mol (docking score). For visualization and analysis of docking results, PyMOL molecular viewer version 1.6 was used. For the prediction of ADMET parameters, automated online program admetSAR was used.[32]

Acknowledgment The authors are thankful to Mr. Shri Manish Ji, NMR department, Sophisticated Analytical Instrumentation Facility (SAIF), Panjab University, Chandigarh, India for recording NMR spectra of the samples.

Conflict of Interest The authors declare no conflict of interest.

Supplementary Materials UV, FT-IR, ^{1}H-NMR, and HR-MS spectra of all the compounds (**3**–**10**) are provided as supplementary material.

References

1) Lerner A. B., Fitzpatrick T. B., Calkins E., Summerson W. H., *J. Biol. Chem.*, **187**, 793–802 (1950).
2) Mason H. S., *Adv. Enzymol. Relat. Subj. Biochem.*, **16**, 105–184 (1955).
3) Iozumi K., Hoganson G. E., Pennella R., Everett M. A., Fuller B. B., *J. Invest. Dermatol.*, **100**, 806–811 (1993).
4) Mosher D. B., Pathak M. A., Fitzpatrick T. B., Eisen A. Z., Wolff K., Freedberg I. M., Austen K. F., "Update: Dermatology in General Medicine," McGraw-Hill, New York, 1983, pp. 205–225.
5) Maeda K., Fukuda M., *J. Soc. Cosmet. Chem.*, **42**, 361–368 (1991).
6) Ha Y. M., Kim J. A., Park Y. J., Park D., Kim J. M., Chung K. W., Lee E. K., Park J. Y., Lee J. Y., Lee H. J., Yoon J. H., Moon H. R., Chung H. Y., *Biochim. Biophys. Acta*, **1810**, 612–619 (2011).
7) Bandgar B. P., Adsul L. K., Chavan H. V., Shringare S. N., Korbad B. L., Jalde S. S., Lonikar S. V., Nile S. H., Shirfule A. L., *Bioorg. Med. Chem.*, **20**, 5649–5657 (2012).
8) Ha Y. M., Park Y. J., Kim J. A., Park D., Park J. Y., Lee H. J., Lee J. Y., Moon H. R., Chung H. Y., *Eur. J. Med. Chem.*, **49**, 245–252 (2012).
9) Kang S. M., Heo S. J., Kim K. N., Lee S. H., Yang H. M., Kim A. D., Jeon Y. J., *Bioorg. Med. Chem.*, **20**, 311–316 (2012).
10) Gawande S. S., Warangkar S. C., Bandgar B. P., Khobragade C. N., *Bioorg. Med. Chem.*, **21**, 2772–2777 (2013).
11) Wang Y., Curtis-Long M. J., Lee B. W., Yuk H. J., Kim D. W., Tan X. F., Park K. H., *Bioorg. Med. Chem.*, **22**, 1115–1120 (2014).
12) Chan C. F., Lai S. T., Guo Y. C., Chen M. J., *Bioorg. Med. Chem.*, **22**, 2809–2815 (2014).
13) Komori Y., Imai M., Yamauchi T., Higashiyama K., Takahashi N., *Bioorg. Med. Chem.*, **22**, 3994–4000 (2014).
14) Solano F., Briganti S., Picardo M., Ghanem G., *Pigment Cell Res.*, **19**, 550–571 (2006).
15) Fujimoto N., Onodera H., Mitsumori K., Tamura T., Maruyama S., Ito A., *Carcinogenesis*, **20**, 1567–1571 (1999).
16) Fisher A. A., *Cutis*, **31**, 240–244, 250 (1983).
17) Seo S. Y., Sharma V. K., Sharma N. J., *Agric. Food Chem.*, **51**, 2837–2853 (2003).
18) Roh J. S., Han J. Y., Kim J. H., Hwang J. K., *Biol. Pharm. Bull.*, **27**, 1976–1978 (2004).
19) Ubeid A. A., Do S., Nye C., Hantash B. M., *Biochim. Biophys. Acta*, **1820**, 1481–1489 (2012).
20) Nabi G., Liu Z. Q., *Bioorg. Med. Chem. Lett.*, **21**, 944–946 (2011).
21) Nagaraju M., Gnana Deepthi E., Ashwini C., Vishnuvardhan M.

V., Lakshma Nayak V., Chandra R., Ramakrishna S., Gawali B. B., *Bioorg. Med. Chem. Lett.*, **22**, 4314–4317 (2012).
22) Herencia F., Ferrándiz M. L., Ubeda A., Domínguez J. N., Charris J. E., Lobo G. M., Alcaraz M. J., *Bioorg. Med. Chem. Lett.*, **8**, 1169–1174 (1998).
23) Suthar S. K., Bansal S., Alam M. M., Jaiswal V., Tiwari A., Chaudhary A., Alex A. T., Joseph A., *Bioorg. Med. Chem. Lett.*, **25**, 5281–5285 (2015).
24) Siddiqui Z. N., Musthafa T. N., Ahmad A., Khan A. U., *Bioorg. Med. Chem. Lett.*, **21**, 2860–2865 (2011).
25) Nerya O., Vaya J., Musa R., Izrael S., Ben-Arie R., Tamir S., *J. Agric. Food Chem.*, **51**, 1201–1207 (2003).
26) Suthar S. K., Aggarwal V., Chauhan M., Sharma A., Bansal S., Sharma M., *Med. Chem. Res.*, **24**, 1331–1341 (2015).
27) Khatib S., Nerya O., Musa R., Shmuel M., Tamir S., Vaya J., *Bioorg. Med. Chem.*, **13**, 433–441 (2005).
28) Jun N., Hong G., Jun K., *Bioorg. Med. Chem.*, **15**, 2396–2402 (2007).
29) Okombi S., Rival D., Bonnet S., Mariotte A. M., Perrier E., Boumendjel A., *J. Med. Chem.*, **49**, 329–333 (2006).
30) Radhakrishnan S., Shimmon R., Conn C., Baker A., *Bioorg. Chem.*, **62**, 117–123 (2015).
31) Lipinski C. A., Lombardo F., Dominy B. W., Feeney P. J., *Adv. Drug Deliv. Rev.*, **46**, 3–26 (2001).
32) Cheng F., Li W., Zhou Y., Shen J., Wu Z., Liu G., Lee P. W., Tang Y., *J. Chem. Inf. Model.*, **52**, 3099–3105 (2012).